SYNTHETIC LUBRICATION

RESEARCH, DEVELOPMENT AND APPLICATION OF SYNTHETIC LUBRICANTS AND FUNCTIONAL FLUIDS

Volume 10, Number 1, April 1993. ISSN 0265-6582

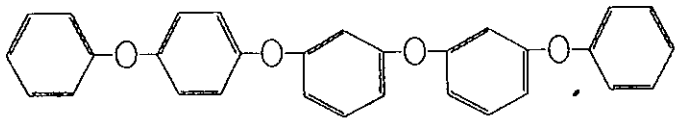

Leaf Coppin

The Film-Forming Properties of Polyalkylene Glycols

M.E. Aderin, G.J. Johnston and H.A. Spikes *Imperial College, University of London, GB* **T.G. Balson and M.G. Emery** *Dow Chemicals Company, Horgen, Switzerland*

It is now recognised that, for many practical applications, an important property of a lubricant is its ability to generate thick, elastohydrodynamic (EHD) films in concentrated contacts. This paper describes a study of the EHD film-forming properties of polyalkylene glycol lubricants. A wide range of polyglycol structures have been examined, with different monomer types, initiators, and molecular weights. Film thickness has been measured at several different temperatures using both conventional and ultra-thin film interferometry. From the measured film thicknesses, the effective pressure–viscosity coefficients of the lubricants have been evaluated. This has enabled a systematic investigation of the effect of polyalkylene glycol structure on both pressure–viscosity coefficient and EHD film formation.

KEYWORDS: *elastohydrodynamic, film thickness, polyalkylene glycol, butylene oxide, interferometry, pressure–viscosity coefficients*

INTRODUCTION

Polyalkylene glycols are an important group of lubricants, which are finding increasing use in practical systems, such as transmissions and hydraulics. They are attractive in this context since they possess a combination of high viscosity index with low coefficient of friction or traction, implying low power loss, and they also demonstrate clean burn-off and, therefore, little tendency to form deposits. Selection of appropriate molecular chain-repeating unit and chain-length permits control of both their polarity and their viscosity characteristics, and a range of base stocks from water soluble to mineral oil soluble are available.

Although polyglycols have been available for some years, very little information exists about their ability to generate elastohydrodynamic (EHD) films under the conditions of high pressure and shear rate prevailing in operating contacts. the aims of the current work were two-fold. Firstly, to provide

JSL 10-1 23 0265-6582 $7.00 + $2.50

primary data for use in predicting film formation by polyglycol lubricants in engineering applications. Of particular interest in this context was the performance of a new range of polyglycol lubricants, based upon butylene oxide. Secondly, the aim was to develop further understanding of the relationship between molecular structure and film-forming ability by looking at a well-characterised set of different polyglycol lubricant structures.

This work thus consists of a systematic study of the elastohydrodynamic film-forming ability of a wide range of polyglycol types at a range of conditions. EHD film thickness was measured using a combination of conventional optical interferometry and, for high temperature work, ultra-thin film interferometry, a new technique able to measure the thickness of very thin films in contacts.

This paper first describes the basis of elastohydrodynamic lubrication and examines briefly the few previous research studies of the behaviour of polyglycols as lubricants to have appeared in the literature. The experimental techniques and results of the current work are then described. Finally, the results and the relationship between polyglycol structure and film-forming ability are discussed.

BACKGROUND

Elastohydrodynamic film formation

Elastohydrodynamic (EHD) lubrication occurs between loaded, rubbing, non-conforming surfaces as found in many mechanical systems such as gears and rolling element bearings. In such systems, very high pressures, typically 1 to 3 GPa in magnitude, are produced in contacts and these have two important effects. Firstly, they result in local elastic deformation of the surfaces, to produce a small, flattened contact zone, typically 0.1 to 1 mm across for steel surfaces. Secondly, the high pressure causes the viscosity of the oil in the contact inlet to increase to many times its normal, atmospheric-pressure value. These two effects couple and, at moderate rubbing speeds, result in the formation of an 'elastohydrodynamic' oil film between the surfaces. In such contacts, the conditions experienced by the lubricant are extreme, involving not just very high pressures but also high shear rates of typically 10^6-10^7 s^{-1} in the inlet zone.

In recent years, appreciation has grown of the importance of being able to calculate and predict EHD film thickness in engineering systems. These film

thicknesses are of the same order as the surface roughnesses of many transmission components and the ratio of film thickness to surface roughness, often called the λ-value, is a valuable measure of the severity of EHD contact operating conditions. For λ-values above 2, negligible solid-solid contact takes place through the film whereas for λ-values below 0.5 there is considerable solid-solid interaction so that surface damage may result.

Most theoretical and experimental determinations of film thickness lead to relationships for EHD oil film thickness, h, of the form:

$$\frac{h}{R'} = k\left(\frac{U\eta_o}{E'R'}\right)^a (\alpha E')^b \left(\frac{W}{E'R'^2}\right)^c \qquad (1)$$

Here E' and R' are the reduced Young's modulus and reduced radius of the interacting solids and W and U are the applied load and the mean speed, $(U_1+U_2)/2$, of the two surfaces. a, b, and c are constants and most workers assign values of between 0.6 and 0.8 to a, between 0.5 and 0.6 to b and around –0.1 to c.[1] The value of k depends upon the overall geometry of the two surfaces and thus of the contact. η_o and α are, respectively, the viscosity at atmospheric pressure and the pressure–viscosity coefficient of the lubricant at the prevailing inlet temperature and shear rate. The pressure–viscosity coefficient α is defined by

$$\frac{d}{dP}(ln\eta)$$

Elastohydrodynamic film thicknesses can thus be calculated, using eq. (1), so long as α and η_o are known for the lubricant in question. In principle, both can be measured using conventional viscometry but there are complications, especially since the values are required to be at high shear rate conditions. It has often been convenient to determine effective pressure–viscosity coefficients of lubricants for use in eq. (1) not by high pressure viscometry, but by measuring elastohydrodynamic film thickness in a test rig and then using this, in conjunction with eq. (1), to determine pressure–viscosity coefficient. This is the approach employed in the current work.

The pressure–viscosity coefficients of most lubricants lie between 5 and 35 GPa^{-1} at room temperature (for all known fluids, α falls with increasing temperature).[2] A number of studies have examined the general relationship between film-formation and molecular structure. These have shown that lubricants based upon molecules with a large degree of internal flexibility, such as

silicones, polyglycols, and esters, tend to have low α-values, as do very simple, symmetrical molecules such as benzene. Alicyclic rings and bulky, relatively rigid molecules whose structural sub-units cannot easily rotate usually have higher α-values. Eq. (1) implies that the highest possible α-value is desirable. However, there is a competing requirement that makes this impracticable. Lubricants generally need to operate at a range of temperatures which requires that they should retain a useful viscosity over this range. This means that they must possess a low temperature–viscosity coefficient

$$\gamma = \frac{d}{dT}(ln\eta)$$

Unfortunately there is a broad correlation between the temperature– and pressure–viscosity coefficients, which implies that a lubricant with a high pressure–viscosity coefficient, desirable for EHD, will also have a high temperature–viscosity coefficient. Recently it has been shown that this correlation has a thermodynamic basis and that there is some scope for optimisation, since fluids with a low internal pressure will have a high ratio of pressure– to temperature–viscosity coefficient.[3]

The current paper describes results of measurements of both pressure– and temperature–viscosity coefficient for a range of well-characterised polyglycol lubricants at a range of temperatures. Pressure–viscosity coefficients were determined from optical interferometric film thickness measurements in an elastohydrodynamic contact and temperature–viscosity coefficients were calculated from conventional viscometry.

Polyalkylene glycols

Polyalkylene glycols – preparation, nomenclature, and structure Polyalkylene glycols are generally prepared by S_N2 base catalysed cleavage of

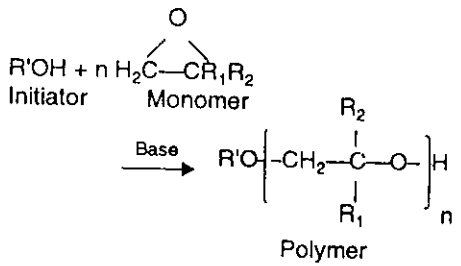

(2)

alkylene oxides (epoxides) according to reaction scheme (2) above. The position at which the initiator and, subsequently, the extending chain attack the monomer is determined by steric factors, with attack occurring at the least hindered carbon.

Table 1 details the initiators and epoxides used in the current study. The letters in brackets are the abbreviated nomenclature used throughout this paper. The co-polymers used in this work (see below, page 35, Test lubricants) are of a random, rather than a block type. The initiators (B), (D), and (T) were chosen so that the role of the functionality of the initiator, of 1, 2, and 3 respectively, could be examined.

Table 1 Nomenclature of monomers and initiators used in current study

Initiator	*Monomer*
(B) $CH_3(CH_2)_2CH_2OH$	(EO) $R_1 = R_2 = H$
(D) $O(CH_2.HCH_3COH)_2$	(PO) $R_1 = H$; $R_2 = CH_3$
(T) $CH_2OHCH(OH)CH_2OH$	(BO) $R_1 = H$; $R_2 = CH_2CH_3$

Polyalkylene glycols – previous use in lubrication The only detailed study reported in the literature of the effects of molecular structure on the lubricating ability of polyglycols was conducted by Kussi.[4] The following section outlines this work together with previous studies that have touched upon the subject.

1. Rheological properties The results of Kussi[4] are summarised in **Table 2**. In this table, 1 indicates the highest and 7 the lowest α-value or VI. THF represents tetrahydrofuran; BO+ represents $R_2 = (CH_2)_{n'}CH_3$, where $n' \geq 1$. The range of polyglycols tested was found to have flatter temperature–viscosity curves, that is higher viscosity indices (VIs) or lower temperature–viscosity coefficients, than mineral oils. The VI was found to increase with EO content in EO:PO co-polymers. Polymers containing branches in mid-chain, resulting from increased functionality of the initiator, showed reduced VI, but these were still much higher than for high VI mineral oils.

The polyglycols tested were found to have lower pressure–viscosity coefficients or α-values than mineral oils. **Table 2** demonstrates that the relative α-values have the following dependence on structure:

Table 2 Dependence of α and VI on chain structure, after Kussi[4]

α	VI	Chain monomers	(R) Random (BK) Block	(L) Linear (B) Branched
1	2	PO	-	L
2	3	EO:PO	R	L
3	4	PO	-	B
4	7	EO:PO:THF:BO+	R	L
5	5	EO:PO	R	B
6	1	EO:PO	BK	L
7	6	EO:PO:THF	R	L

(i) PO > PO:EO and linear > branched;
(ii) for PO:EO co-polymers R > BK and linear > branched;
(iii) chain monomer type is more important than linear/branched chain type.

Similar behaviour was observed by Geymayer,[5] who compared two mineral oils (A and B) and a number of polyglycols (initiator = H_2O) with viscosities of approximately 0.1 Pa.s at atmospheric pressure. **Table 3** summarises the approximate α-values which were calculated from figures in reference (5).

Table 3 Pressure–viscosity coefficients calculated from reference (5)

Oil 4	α/GPa^{-1}
Mineral oil A	33
Mineral oil B	21
PO	16.5
PO:EO = 1:1	12.5
PO:EO = 1:4	10.5

Table 4 consists of a summary of various polyglycol α-values found in the literature. It shows the dependence of α on temperature. Glycerol, an initiator used in the current study, is included for comparison.

Table 4 Pressure–viscosity coefficients of polyglycols from the literature

Lubricant	Ref.	α/GPa^{-1} Temperature/°C			
		25	30	60	100
EO:PO co-polymer	(6)	-	17.6	14.3	12.2
PO 750	(6)	-	17.8	-	-
PO 1500	(6)	-	17.4	-	-
UCON LB 165	(7)	14	-	-	-
Glycerol	(6)	-	5.9	5.5	3.6

2. Friction and wear properties Geymayer[5] compared the wear rates in an FZG test for an unformulated mineral oil and an additive-free, 1:1 EO:PO polyglycol, i.e. one built from 50% wt. EO and 50% wt. PO monomers. Much lower wear was observed with the polyglycol. Kussi[4] investigated the wear behaviour of the lubricants shown in **Table 2** in both boundary and full fluid-film EHD lubrication regimes. In all cases the polyglycols produced lower friction and wear than a mineral oil of similar viscosity. EO:PO co-polymers tested in boundary lubrication demonstrated improved friction and wear as the EO content was increased. Pure POs showed poorer friction and wear than EO:PO co-polymers. Larger monomer units improved this behaviour. A roller-bearing rig (EHD regime) was employed to investigate traction losses. Polyglycols were shown to be more efficient than a mineral oil, both with and without an additive-package. A range of tests carried out on mixtures of the oil soluble polyglycol (EO:PO:THF:BO+) in mineral oil demonstrated improved friction, wear, and traction losses as the polyglycol concentration was increased.

Finally, Kussi[4] has shown that increased thermal stability results both from the use of larger monomer units and longer overall chain lengths. Suitable stabilisers improve the thermal stability further, up to the temperature at which pyrolysis occurs (240-250°C). This temperature represents a practical maximum for polyglycols.

EXPERIMENTAL TECHNIQUES AND MATERIALS

Film thickness measurements

Film thickness measurements in rolling EHD contacts were made in the current study using two techniques: conventional, monochromatic interferometry and a new technique, ultra-thin film optical interferometry. The principle of the latter can be most clearly explained by comparison with the former.

Conventional optical interferometric method The principle of conventional interferometry as applied to EHD is shown in **Figure 1**. The contact consists of a reflective, smooth steel ball loaded against a rotating, flat, transparent glass disc. Light is shone into the contact through the glass. Some of this light is reflected from the underside of the glass disc and some passes through any oil film and is then reflected back from the steel ball. Since the two beams of light have travelled different distances they interfere according to the rules:

Constructive interference:

$$h_{oil} = \frac{(N - \phi)\lambda}{2n\cos\theta} N = 1, 2, 3... \quad (3)$$

Destructive interference:

$$h_{oil} = \frac{(N + \frac{1}{2} - \phi)\lambda}{2n\cos\theta} N = 0, 1, 2... \quad (4)$$

λ is the wavelength of the light that interferes, N is the fringe order, n the refractive index of the film and ϕ a phase change that is characteristic of the surfaces and takes place upon reflection. For optimum clarity of interference the two light beams should have similar intensity and this is achieved by applying a semi-reflective coating of chromium to the underside of the transparent flat, as shown in **Figure 1**.

If monochromatic light is employed, a series of dark and light fringes is seen, each fringe corresponding to a particular separation in accordance with eqs. (3) and (4). If white light is used, then at any given separation a certain wavelength of the light will constructively interfere and another destructively

Figure 1 Basic interferometric method (two beam)

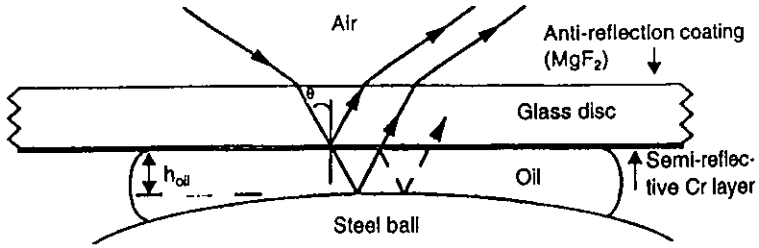

interfere. The result will be a complex series of coloured fringes which, after calibration, can be related to separation.[1]

Ultra-thin film technique The ultra-thin film system is based around two advances to conventional optical interferometry.

A major limitation of the conventional interference approach is that it cannot be used to measure films that are less than approximately one quarter the wavelength of the visible light used, a limit of about 80 nm, since this corresponds to the occurrence of the first destructive interference fringe. To overcome this limitation the ultra-thin film approach uses a transparent, solid, 'spacer layer' coating, applied on top of the semi-reflecting film on the transparent flat, as shown in **Figure 2**. the presence of this coating enables interference fringes to be obtained even in the absence of an oil film since the spacer layer behaves like a permanent, solid coating of oil.

Figure 2 Spacer layer method

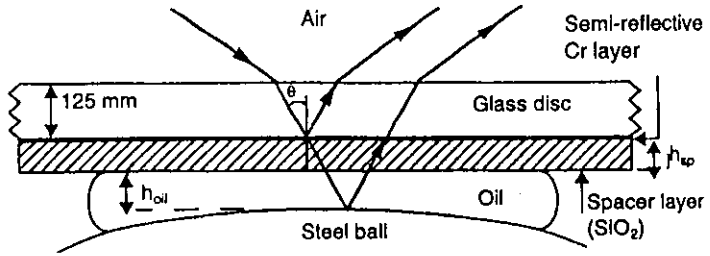

A second limitation of conventional optical interferometry is that only a few, quite widely spaced film thicknesses can be easily measured, so that resolution is poor. For monochromatic interferometry, an interference fringe is produced at every half wavelength separation. For chromatic interferometry using white light, the resolution depends upon the ability of the human eye to remember and distinguish colours and is typically 1/8 of the wavelength of light.

In the ultra-thin film technique a white light source is used and a spectrometer employed in place of the human eye to disperse the light reflected from the contact so that it is possible to determine precisely which wavelengths have been constructively or destructively interfered.

The combination of these two techniques forms the basis of the ultra-thin film technique.[9] The wavelength at which constructive interference occurs is where the film thickness is measured, using a spectrometer, for both a spacer layer alone and for a spacer layer/oil film combination. Oil film thickness is then determined by the following analysis: constructive interference of combined oil and spacer layer for $\theta = 0°$:

$$n_{oil}h_{oil} + n_{sp}h_{sp} = \frac{(N-\phi)\lambda_{sp+oil}}{2} N = 1, 2, 3.... \quad (5)$$

A similar expression can be derived for the spacer layer alone:

$$n_{sp}h_{sp} = \frac{(N-\phi)\lambda_{sp}}{2} N = 1, 2, 3.... \quad (6)$$

Rearranging eqs. (5) and (6) gives an expression for the oil film thickness alone:

$$h_{oil} = \frac{(N_{sp+oil}\lambda_{sp+oil} - N_{sp}\lambda_{sp})}{2n_{oil}} \quad (7)$$

where λ_{sp} and N_{sp} are the measured wavelength of maximum constructive interference and corresponding fringe order for the spacer layer alone, without

Figure 3 Schematic diagram of high-temperature optical rig

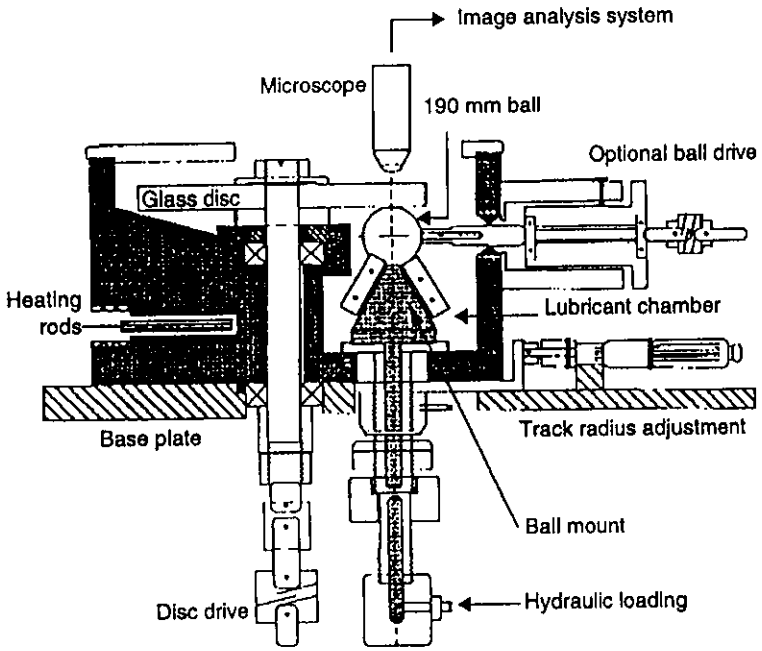

oil. λ_{sp+oil} and N_{sp+oil} are similar values when oil is present. n_{oil} is the refractive index of oil in the contact. All these values can be measured.

Film thickness measurement test details **Figure 3** shows a diagram of the test apparatus used in the current study to measure film thickness. The flat surface of a glass disc was loaded and rotated in nominally pure rolling contact against a 190 mm diameter AISI 52100 steel ball. The disc surface was coated with a 20 nm thick chromium layer and, for the ultra-thin film interferometric tests, a silica spacer layer of thickness approximately 500 nm was deposited on top of this. The load applied was 53 N, corresponding to a maximum Hertz contact pressure of 0.71 GPa.

Refractive index measurement

Refractive indices of the oils tested were measured using a conventional Abbé refractometer. These refractive indices are needed to calculate true spatial film thicknesses as shown in eq. (7). In this study the effect of contact pressure on the refractive index of the lubricant has been neglected. In general, this is likely to result in a systematic over-estimate of film thicknesses measured by about 4%. Since the pressure–viscosity coefficients are determined by comparing film formation with that of a reference oil, as described in the next section, the effect of neglecting the influence of pressure on refractive index should largely be cancelled out.

Table 5 List of polyalkyleneglycol fluids used

Name	*% EO*	*% PO*	*% BO*	*η (20°C)/ cP*
25-50B	75	25	-	190
25-300B	75	25	-	1270
50-50B	50	50	-	151
50-155B	50	50	-	644
100-20B	-	100	-	70
100-30B	-	100	-	86
100-50B	-	100	-	180
100-85B	-	100	-	364
100-150B	-	100	-	604
100-20D	-	100	-	65
BO-50B	-	-	100	239
BO-110B	-	-	100	559
BO-150B	-	-	100	744
BO-130D	-	-	100	573
BO-100T	-	-	100	1247

Dynamic viscosity measurement

For each lubricant tested, dynamic viscosities were measured at the temperatures of interest, using a Ferranti-Shirley cone on plate viscometer.

Test lubricants

Table 5 summarises the test lubricants employed in this study, together with their viscosities at 20°C. As can be seen in this table, four different structural classes of fluid were examined, ethylene oxide(EO)/propylene oxide(PO) copolymers with respectively 25% wt. and 50% wt. PO monomers, polymers based on 100% propylene oxide (PO) and polymers based on butylene oxide (BO). Two or three different viscosity fluids from each of these four categories were tested at four temperatures, to provide a broad overview of the dependence of film-forming properties on monomer type. To look more closely at the influence of structural detail on film formation, tests were also carried out at room temperature on a range of different viscosity fluids of the same monomer class and also on three fluids with different initiators.

In this paper each fluid name has three parts. The first is either a number, to indicate the percentage PO in EO/PO copolymers or is BO if the fluid was made entirely from butylene oxide monomer. The number after the hyphen is the approximate viscosity in cSt at 50°C. The last letter indicates the initiator type, as listed in **Table 1**.

RESULTS AND ANALYSIS

Viscosities and refractive indices

Table 6 shows the measured refractive indices of the polyglycols tested and also their viscosity–temperature characteristics. The latter are expressed in terms of their Vogel coefficients, A, B, C used in the viscosity–temperature equation:

$$\eta = Ae^{B/(T-C)} \tag{8}$$

where η is the dynamic viscosity in cP at temperature T in degrees Kelvin. These coefficients were derived by fitting a regression curve through measured viscosity–temperature data for each fluid.

Table 6 Refractive indices and viscosity characteristics of fluids tested

Name	*RI (20°C)*	*A*	*B*	*C*
25-50B	1.4618	0.270	835	166
25-300B	1.4660	1.349	881	165
50-50B	1.4587	0.906	480	199
50-155B	1.4624	0.179	1264	139
100-20B	1.4488	0.128	774	170
100-30B	1.4493	0.255	629	185
100-50B	1.4516	0.217	808	173
100-85B	1.4528	0.481	743	181
100-150B	1.4534	0.405	894	171
100-20D	1.4510	0.099	707	191
BO-50B	1.4537	0.178	753	189
BO-110B	1.4540	0.279	808	187
BO-150B	1.4543	0.328	829	186
BO-130D	1.4558	0.020	1780	120
BO-100T	1.4527	0.025	1019	199

Typical film thickness results

Figure 4 shows typical measured film thicknesses for one of the fluids tested at four different temperatures. The results are plotted as log (central film thickness) versus log (rolling speed) and, as expected from eq. (1), this type of plot gives a straight line of gradient approximately 0.7. In this figure, the rolling speed required to produce a given film thickness increases with fluid temperature since both viscosity and pressure–viscosity coefficient decrease as the temperature is raised. **Figure 5** shows similar plots for a set of fluids of different type but with similar viscosities, all tested at room temperature.

Figure 4 Log (separation) v log (rolling speed) for 100-50B at a range of temperatures

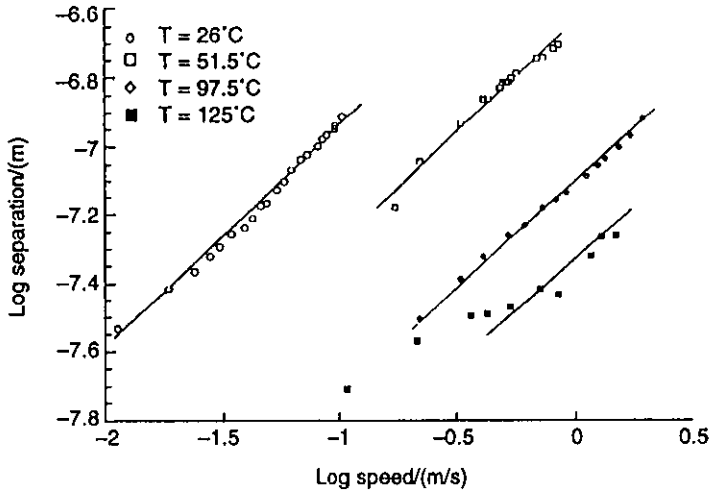

Figure 5 Log (separation) v log (rolling speed) for viscosity matched fluids

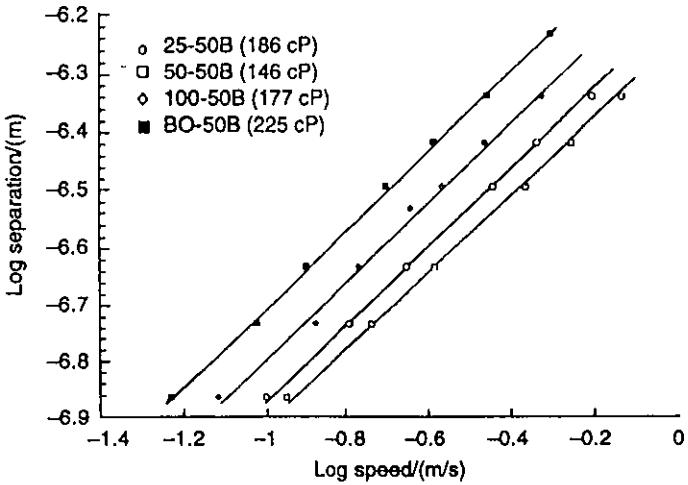

Methods of calculating pressure– and temperature–viscosity coefficients

Film thickness regression equations such as eq. (1) predict that central film thickness should be proportional to the effective pressure–viscosity coefficient, α, raised to the power 0.53. To calculate α in this study, the standard method described by Foord was employed.[8] Log(h) was plotted for each lubricant against log ($U\eta$), where η is the lubricant's dynamic viscosity at the test temperature and atmospheric pressure. On the same graph was also plotted log(h) versus log($U\eta$), using the same viscosity, speed, and film thickness units, for a reference oil of known pressure–viscosity coefficient, α. Based on eq. (1), any difference in film thickness at fixed $U\eta$ for the two fluids tested under the same conditions should result from a difference in α. The central film thicknesses produced by both the test oil h_t and the reference oil h_r at the same, fixed, value of $U\eta$ were therefore taken from the graph and compared.

The pressure–viscosity coefficient of the test oil, α_t, could be worked out from these two values and the known pressure–viscosity coefficient of the reference oil, α_r, using eq. (9):

$$\frac{h_t}{h_r} = \frac{\alpha_t^{0.53}}{\alpha_r^{0.53}} \qquad (9)$$

The advantage of this technique over employing a full film thickness regression equation is that it makes less assumptions as to the accuracy of the latter. By comparing a test and reference oil under identical conditions, no assumptions are made about the effect of any of the known independent variables, W, E, R, $U\eta$, on film thickness, only about the influence of α thereon.

Calculated pressure and temperature–viscosity coefficients

Figure 6 shows the film thickness/speed data from **Figure 4** plotted as log (film thickness) versus log ($U\eta$). This brings closer together the different temperature results since it eliminates the effect of variations in bulk viscosity on film thickness, leaving only the residual effect of the differences in pressure–viscosity coefficient, α, at different temperatures, enabling the latter to be determined.

Pressure–viscosity coefficients were calculated in this way for all the fluids tested. **Figures 7, 8,** and **9** (see overleaf) show curves of how pressure–

Figure 6 Log (separation) v log (rolling speed x viscosity) for 100-50B at a range of temperatures

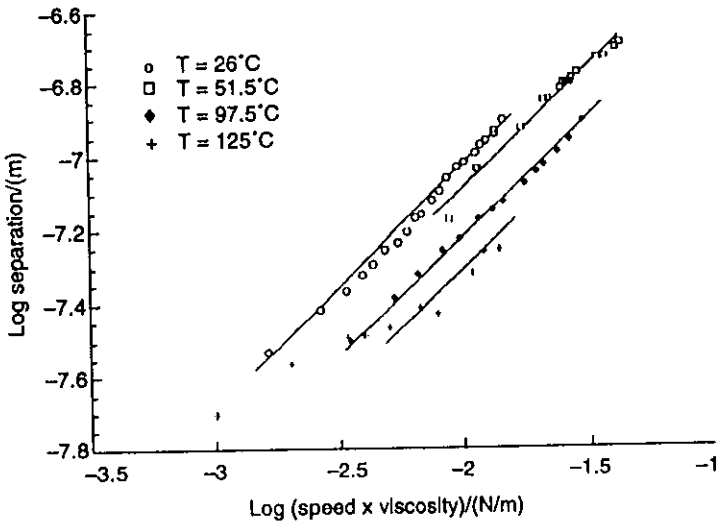

viscosity coefficient varies with temperature and **Table 7** (see overleaf) lists measured room temperature values.

DISCUSSION

The pressure–viscosity coefficients measured in this study are similar to the few values reported in the literature by other workers. The α-value/temperature plots are broadly as expected, showing a fall with temperature with a levelling off at high temperatures.[10]

The room temperature results enable the effects of various structural parameters on pressure–viscosity coefficient to be observed. **Figure 10** (page 42) compares five different monomer systems. The first four of these are chosen to have approximately the same viscosity and the first three and the last have almost the same chain length, i.e. the same number of monomer units in the average chain. As the proportion of propylene to ethylene increases, so the pressure–viscosity coefficient rises. This is in accord with earlier work with polyglycols.[5] The trend continues with the butylene system which has the largest α-value. Similar effects have been observed in the past when comparing

Figure 7 Effective pressure–viscosity coefficients of EO:PO Copolymers at a range of temperatures

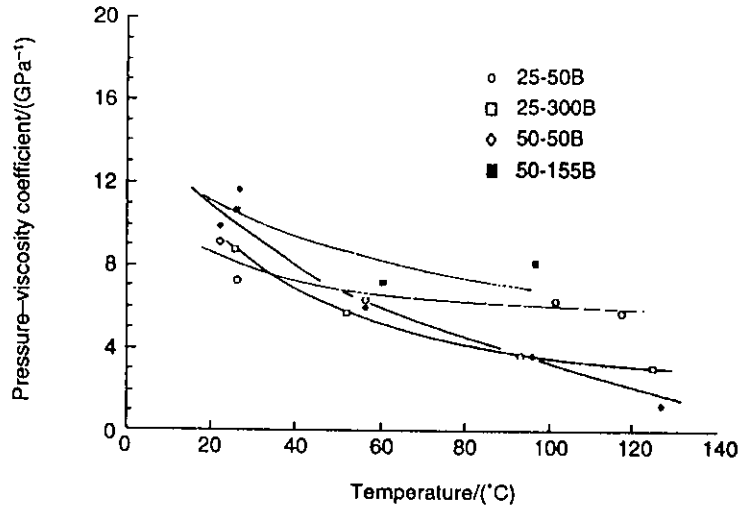

Figure 8 Effective pressure–viscosity coefficients of 100% PO polymers at a range of temperatures

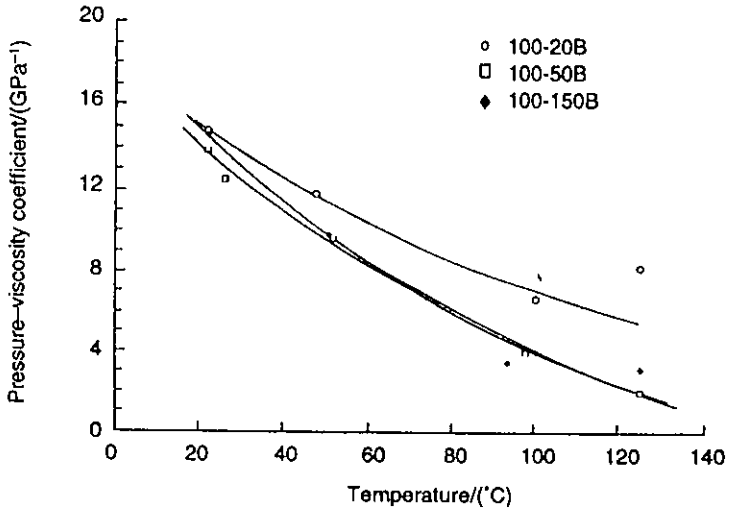

Figure 9 Effective pressure–viscosity coefficients of 100% BO polymers at a range of temperatures

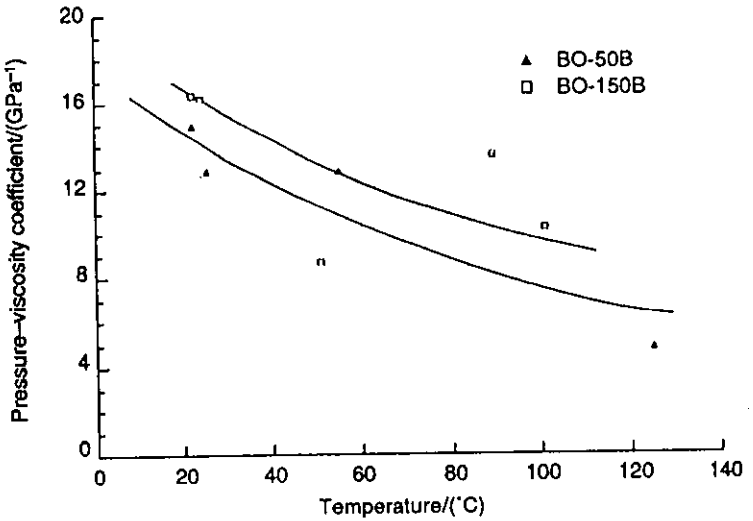

perfluorinated propylene and methylene/ethylene ethers.[7] In general it appears that the presence of a large number of short side chains has the effect of raising

Table 7 Effective pressure–viscosity coefficients of fluids tested at 22°C

Name	*α (22°C)/GPa⁻¹*
25-50B	9.1
50-50B	9.9
100-20B	14.8
100-30B	13.5
100-50B	13.9
100-85B	14.3
100-150B	14.6
100-20D	14.8
BO-50B	14.9
BO-110B	15.7
BO-130D	15.2
BO-100T	7.7

Figure 10 Effective pressure–viscosity coefficients of similar viscosity and average chain length polymers at 22°C

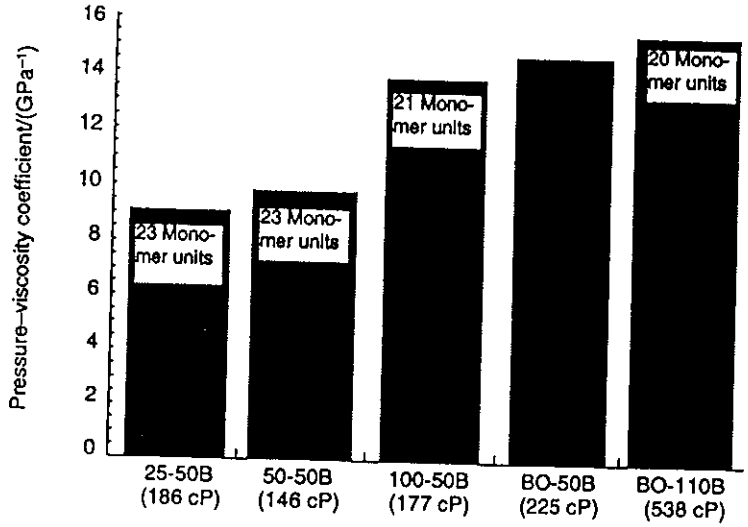

Figure 11 Influence of viscosity on effective pressure–viscosity coefficients for 100% PO polymers at 22°C

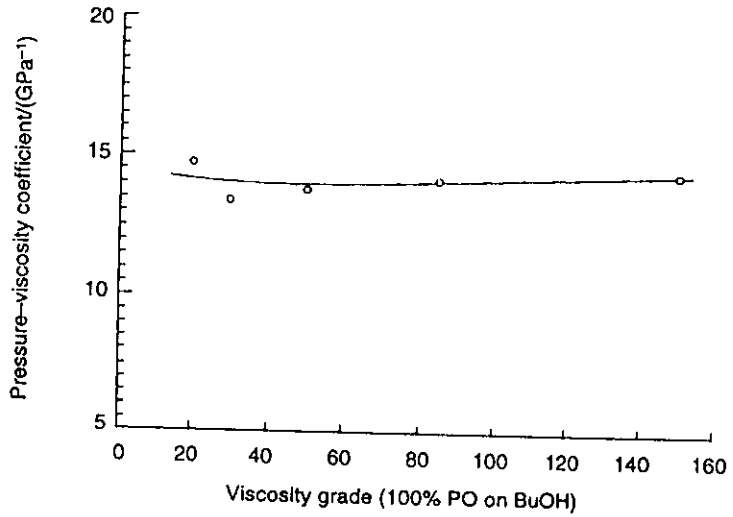

pressure–viscosity coefficient. It is not yet known what happens as the side chain length progressively increases. It is likely that as this occurs, the α-value will level out at a value representative of alkanes and polyalphaolefins, typically 10-15 GPa^{-1} at room temperature.

Figure 11 shows the effect of increasing molecular weight and thus viscosity. The pressure–viscosity coefficient is only weakly dependent upon viscosity at room temperature. This has also been seen with perfluoropolyethers.[7] Some of the results taken over a range of temperatures indicate that at intermediate to high temperatures there may, however, be a greater dependence of α-value on viscosity than at room temperature.

The effect of using initiators with different functionalities can be seen in **Figure 12.** The only initiator which seems to give a significantly different pressure–viscosity coefficient from the others is glycerol, with a functionality of three. The reason for the lower α-value for this fluid is not clear, but may be related to incomplete alkoxylation of the secondary hydroxyl group on the initiator.

Figure 13 (see overleaf) shows a plot of pressure–viscosity coefficient versus temperature–viscosity coefficient for all the fluids tested in this study. The general correlation between the two properties can be clearly seen.

Figure 12 Influence of initiator type on effective pressure–viscosity coefficients at 22°C

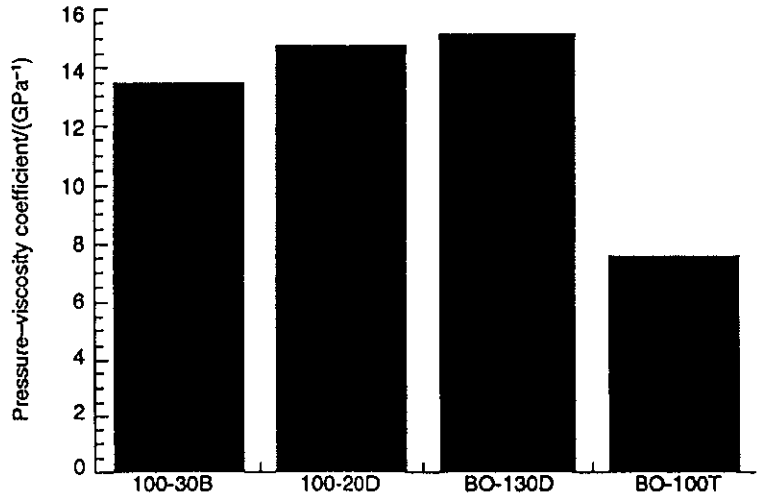

Figure 13 Plot of pressure–viscosity versus temperature–viscosity coefficient for all the fluids tested

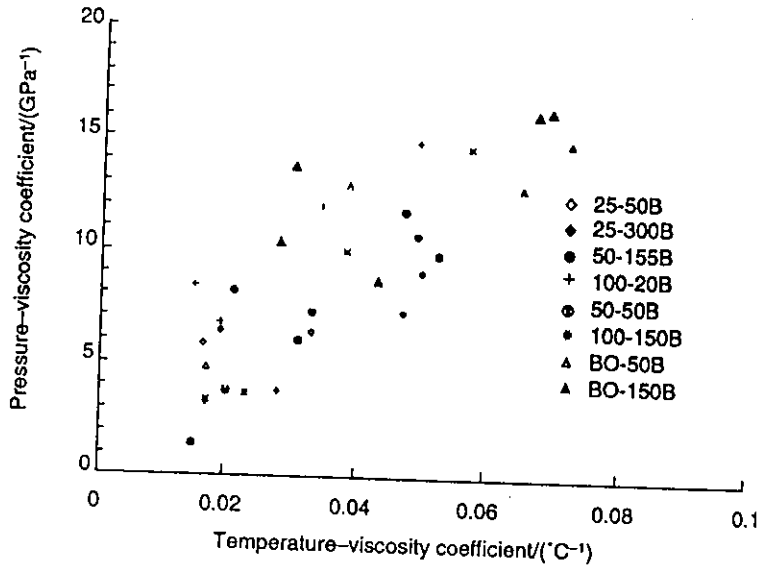

CONCLUSIONS

The elastohydrodynamic film-forming properties of a range of polyalkylene glycols have been measured using interferometry at several temperatures up to 125°C and from these, the effective pressure –viscosity coefficients of the fluids have been determined. Pressure–viscosity coefficient increases with increasing proportion of branched chain alkylene monomer. Butylene-based polyglycols give pressure–viscosity coefficients higher than those of propylene-based ones. The molecular weight and thus viscosity of the polyglycol has little effect on pressure–viscosity coefficient, nor, in most cases, does the polymerisation initiator.

ACKNOWLEDGEMENTS

The authors would like to thank the Dow Chemicals Company for the supply of polyglycol lubricants and for enabling this study to take place.

References

1. Dowson, D., and Hamrock, B.T., *Ball Bearing Lubrication. The Elastohydrodynamics of Elliptical Contacts*, J. Wiley & Sons (1981).
2. Jones, W.R., Johnson, R.L., Winer, W.O., and Sanborn, D.M., 'Pressure–viscosity measurements of several lubricants to 5.5 x10⁸ N/m² and 149°C', *ASLE Trans.*, 18, 4, 249-62 (1975).
3. Spikes, H.A., 'A thermodynamic approach to viscosity', *STLE Trans.*, 33, 1, 141-8 (1990).
4. Kussi, S., 'Chemical, physical, and technological properties of polyethers as synthetic lubricants', *J. Synth. Lubr.*, 2, 1, 63-84 (1985).
5. Geymayer, S., 'Polyalkylenglykole', in Synthetic Lubricants and Operational Fluids, 4th International Coll., Technische Akademie Esslingen, 3.1-3.6 (1984).
6. Gohar, R., 'Elastohydrodynamics', Ellis Horwood Ltd., J. Wiley & Sons (1988).
7. Spikes, H.A., Cann, P., and Caporiccio, G., 'Elastohydrodynamic film thickness measurements of perfluoropolyether fluids', *J. Synth. Lubr.*, 1, 1, 73-86 (1984).
8. Foord, C.A., Hamman, W.C., and Cameron, A., 'Evaluation of lubricants using optical elastohydrodynamics', *ASLE Trans.*, 11, 1, 31-43 (1968).
9. Johnston, G.J., Wayte, R., and Spikes, H.A., 'The measurement and study of very thin lubricant films in concentrated contacts', *STLE Trans.*, 34, 187-94 (1991).
10. Mobil EHD Guidebook, Mobil Oil Company, 1979.